Metallomics

Accepted Manuscript

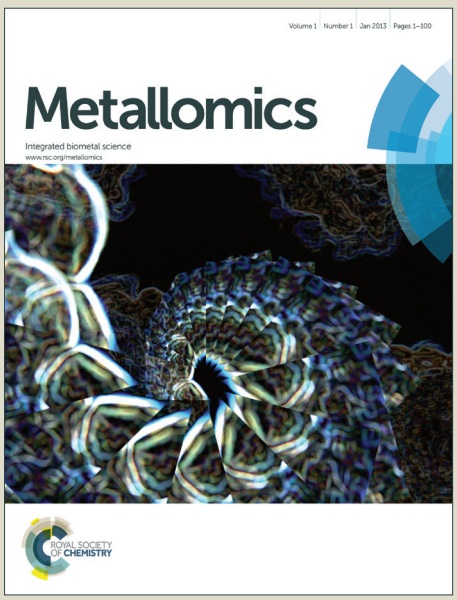

ROYAL SOCIETY OF CHEMISTRY

www.rsc.org/metallomics

Distributions of iron, phosphorus and sulfur along trichomes of the cyanobacteria *Trichodesmium*

Jochen Nuester[a,*] , Matthew Newville[b], and Benjamin S. Twining[a]

[a]Bigelow Laboratory for Ocean Sciences, 60 Bigelow Drive, East Boothbay, Maine 04544, USA

[b]Center for Advanced Radiation Sources, The University of Chicago, Argonne, IL, USA

*corresponding author: jnuester@bigelow.org

ACKNOWLEDGEMENTS: This work was supported by grants from the US National Science Foundation to BST (OCE-0913080, OCE-1061545). Use of the Advanced Photon Source, an Office of Science User Facility operated for the U.S. Department of Energy (DOE) Office of Science by Argonne National Laboratory, was supported by the U.S. DOE under Contract No. DE-AC02-06CH11357.

Abstract

The nonheterocystous cyanobacterium *Trichodesmium* fixes C and N concurrently during the light period in tropical and subtropical oceans. Synchrotron mapping of Fe, P and S in trichomes of *Trichodesmium erythraeum* Erhenberg IMS 101 (CCMP 1985) collected during exponential and senescent growth revealed that 16 % of trichomes contained sections of up to 25 cells with ca. 2-fold elevated Fe and S but ca. 2-fold less P in comparison to neighboring trichome sections. The correlation between Fe and S in these trichomes was moderate to strongly positive ($R>0.35$), while the correlation between Fe and P was moderate to strongly negative ($R<0.35$). Higher Fe in theses trichome sections might indicate the presence of nitrogenase. Increase in S in conjunction with Fe is likely driven by other S-containing compounds in addition to Fe-S proteins. Furthermore, the concurrent increase in S and decrease in P in these Fe-rich trichome sections might indicate a switch from P- to S-containing compounds. Diurnal changes and growth phase-related differences in the correlation between Fe and P both point to *Trichodesmium*'s ability to re-allocate elements depending on their physiological need. Concurrent P depletion and Fe and S enrichment in trichome sections is a strong indication that *Trichodesmium* is able to develop special trichome regions consisting of multiple cells with a unique chemical composition. Whether these cells are uniquely dedicated to N-fixation (ie, diazocytes) is an open question.

Introduction

The topic of climate change has elevated attention to the processes that sequester atmospheric CO_2 in the upper water column. N_2-fixation, the conversion of N_2 gas into ammonia, accounts for around one half of the input of biological available N to the ocean[1] and enables the sequestration of atmospheric CO_2 beyond that supported by nitrate alone in the vast areas of the (sub-)tropical and oligotrophic oceans. N_2-fixation is carried out by a small group of organism of which cyanobacteria are the dominant members in open ocean waters, and the cosmopolitan filamentous cyanobacteria of the genus *Trichodesmium* are considered major contributors to this process.[2]

Despite the recognition of the importance of *Trichodesmium* for N_2-fixation and CO_2-sequestration[2], the biochemistry of *Trichodesmium* is still enigmatic, because *Trichodesmium* has a physiological adaptation that allows for C- and N_2-fixation concurrently during the light period, an ability which is otherwise exclusive to heterocystous cyanobacteria.[3] This physiological adaptation is unique because it combines spatial and temporal separation of C- and N_2-fixation to protect the oxygen-sensitive nitrogen-fixing enzyme nitrogenase from oxidative damage by reactive oxygen species (ROS).[4]

Non-uniform distribution of nitrogenase along *Trichodesmium* trichomes detected by immunolocalization led to the proposition of dedicated N-fixing cells (termed diazocytes), analogous to the formation of heterocystous cells. [4a, 4c] These diazocyte cell sections were further identified by electron microscopy[5] and conventional microscopy after Lugols staining.[6] Diazocytes differ from neighboring vegetative cells by a reduced number of storage compounds and gas vacuoles, giving diazocytes a more transparent appearance.[5] Diazocyte-type cells differ from heterocyst cells found in other diazotrophs by lacking a thickened cell envelope and

retaining all compounds of the photosynthetic apparatus.[5] The identification of diazocytes in trichomes is controversial because other studies using similar techniques[7] and as well nanoscale secondary ion mass spectrometry[8] have found even distributions of nitrogenase and C-and N_2-fixation along the entire length of trichomes. The genome of *Trichodesmium* also does not provide evidence supporting the existence of specialized N_2-fixing cells. The *nif* operon of *Trichodesmium* has some similarities to the *nif* operon of heterocystous cyanobacteria, but lacks some key genes such as *hglCDE* and *hepB* involved in the formation of the outer heterocyst envelope.[4b, 9]

In addition to the formation of diazocytes, *Trichodesmium* may also temporally separate N_2- and C-fixation, as well as reduce oxygen evolution through the Mehler reaction, to further protect nitrogenase against oxygen damage.[3a] Berman Frank et al.[3a] found that nitrogenase activity concomitantly increased with enhanced oxygen-scavenging through the Mehler reaction mechanism during mid-day. This depression in oxygen production is expressed as a lower quantum yield (~50%) and a low net oxygen evolution. Fast temporal changes between high fluorescence states in N_2-fixing cells and recovery states during non-N_2-fixing periods of *Trichodesmium* IMS101, and rearrangements of phycobilosomes between PSI and PSII, were also attributed to a nitrogenase-protective mechanism that allows for N_2-fixing activity even in cells lacking thick cells walls.[10] However, as these changes occur within seconds or minutes it was questioned if this timeframe would be sufficient to protect nitrogenase from oxidative damage.[3b]

The nitrogenase enzyme complex is one of the most Fe-rich enzyme complexes in nature.[11] The conventional nitrogenase complex, which is assumed to be expressed in *Trichodesmium,* is a two-component metalloenzyme and consists of MoFe- and Fe-proteins.

Both proteins are assumed to occur in the nitrogenase complex of *Trichodesmium* in a 1:2 stoichiometry.[11-12] Each nitrogenase complex contains 38 Fe atoms, of which 4 are bound to each Fe-protein dimer, and 30 are included in the MoFe protein tetramer. The presence of nitrogenase in *Trichodesmium* is reflected in elevated Fe quotas in comparison to other phytoplankton in both laboratory[13] and field studies.[14] Overall, Whittaker et al.[11] estimated that 236 μmol Fe are contained in nitrogenase per mol cellular C, and Kustka et al.[15] predicted that 19 to 53 % of cellular Fe in *Trichodesmium* is located in nitrogenase. Similarly, nitrogenase expression in *Trichodesmium* results in elevated Mo quotas relative to other phytoplankton.[14, 16] Although the presence of the conventional nitrogenase complex is assumed for *Trichodesmium*, Nuester et al.[14] reported that Trichodesmium can also be enriched in V, an element that typically is associated with an alternative nitrogenase complex in which Mo is replaced by V.[17]

In this study we present data on the spatial distributions on Fe, S, and P along individual trichomes of *Trichodesmium erythraeum* Erhenberg IMS 101 (CCMP 1985) grown under Fe-replete conditions and sampled over the diurnal light cycle in both exponential and stationary phase using synchrotron x-ray fluorescence (SXRF). This spatial and temporal information about the metallome is then linked to the biology of *Trichodesmium*, whereby the distribution of Fe is used as a proxy for the presence of nitrogenase. S and P are used as proxies for other cellular compounds. The spatial relationships between Fe, S, and P during a diurnal cycle is evaluated is the context of diazocyte formation.

Materials and methods

Study organism

Cultures of the marine cyanobacterium *Trichodesmium erythraeum* Erhenberg IMS 101 (CCMP 1985) were obtained from the National Center for Marine Algae and Microbiota (formerly known as Provasoli-Guillard Center for Culture of Marine Phytoplankton, East Boothbay, Maine, USA) and were grown at 31 μmol quanta m^{-2} s^{-1} at 24°C under a 12:12 hour light:dark cycle. The strain was originally isolated from coastal waters of the North Atlantic (35°N, 76°W).

Medium and growth conditions

Trichodesmium was grown in North Atlantic Ocean seawater collected using trace-metal clean techniques in the vicinity of the Bahamas (25° 38.023' N, 77° 26.804' W). The seawater was supplemented with phosphate (50 μmol L^{-1}), vitamins (B_{12} :0.369 nmol L^{-1}, thiamine :296 nmol L^{-1}, and biotin: 2.05 nmol L^{-1}) and modified YBC-II trace metals.[18] The trace metal composition used in this study differs from the original recipe in higher EDTA (100 μmol L^{-1}) and Co (2.5 nmol L^{-1}) and varied Fe concentrations. Iron ($FeCl_3$) was pre-equilibrated with EDTA in a 1 : 1.1 molar ratio and added to achieve final Fe concentrations between 2 and 2000 2000 nmol L^{-1} (Fig. 1). We chose to analyze trichomes from the cultures with the highest Fe concentrations (2000 nmol L^{-1} (Exp. I) and 200 nmol L^{-1} (Exp. II)) in order to maximize rates of N_2-fixation and occurrence of nitrogenase in the trichomes. Trichome counts are not available for the 2000 nmol Fe L^{-1} culture, but the culture was sampled for SXRF after 28 days of growth in conditions similar to those used for 200 nmol Fe L^{-1} culture (other than Fe concentration). We

therefore assume that the trichomes collected from the 2000 nmol Fe L^{-1} culture were in stationary phase when sampled.

Prior to inoculations, the media was filter sterilized using 0.2-μm polycarbonate filter membranes in polysulfone filter holders and transferred into 2-L polycarbonate bottles. A *Trichodesmium* culture pre-acclimated to 200 nmol L^{-1} Fe for 25 days over 3 successive batch cultures was used as inoculum culture for Exps. I, II. All manipulations were carried out using trace-metal clean techniques in a laminar flow hood with labware that was acid-washed in 10% HCl for at least 72 hours and rinsed with ultrapure Q-H_2O (>18 MΩ · cm^{-1}) prior to use.[19]

Synchrotron x-ray fluorescence (SXRF) analysis

Subsamples of *Trichodesmium* were collected for SXRF analysis from cultures at several time points within the diurnal light cycle. *Trichodesmium* was collected for SXRF analysis during senescent growth in Exp. I, and during exponential growth in Exp. II. *Trichodesmium* samples were collected onto 47-mm diameter 2-μm pore-size polycarbonate membranes in polysulfone filter holders, soaked for 15 min in trace-metal clean oxalate reagent,[16b] rinsed 3 times with filtered seawater, re-suspended in 0.8 M trace-metal clean ammonium formate in 50-mL centrifuge tubes, and fixed with 0.5 % trace-metal clean glutaraldehyde.[20] Subsequently, trichomes from each subsample were centrifuged (2,000 × g for 10 min) onto LUXfilm-coated CuTEM support grids (Ted Pella, Redding, Ca). After careful removal of the supernatant, samples were allowed to air dry in a darkened laminar-flow hood and stored in the dark until SXRF analysis.

Element distribution maps of trichome sections (total length of trichomes on grids varied between ca. 30 μm and ca. 1.5 mm) were analyzed using the hard X-ray microprobe beamline

13ID-C at the Advanced Photon Source (Argonne National Laboratory, Argonne, Il, USA). Kirkpatrick-Baez mirrors were used to focus X-rays to a ca. 2 μm spot (FWHM). The samples were placed in a He-filled plastic bag and analyzed using a monochromatic 7.3 keV X-ray beam in order to gain maximum sensitivity for Fe and lower energy elements such as P and S. Trichomes from Exp. I analyzed during a run in October, 2009, and trichomes from the Exp. II were analyzed during a run in July, 2010. Spatial distributions of Fe, S, and P were obtained from two-dimensional element maps and one-dimensional cross sections created by the software package MAPS.[21] X-ray fluorescence expressed in counts per second [CPS] were extracted from pixels belonging to one-dimensional cross sections along the length of each trichome section.

Conversion of X-ray fluorescence data (ie, CPS) to elemental concentrations requires characterization of many variables, including fluorescence yield of the elements, self-absorption of fluorescence X-rays, and fluorescence absorption via the sampling atmosphere and detector windows. These variables were not fully characterized during both runs and therefore it is not possible to calculate absolute areal element concentrations for each run. Thus, here we focus on the relative concentrations of elements within each trichome. However fluorescence signals are directly proportional to element concentrations.[20], and analyses of NBS-certified thin film standards (SRM 1832 and SRM 1833) collected during each run allow us to estimate the relative sensitivity of the microprobe for each element during each run.[22] This comparison indicates that the microprobe sensitivity was approximately 180 and 90 times higher for Fe than for P and S, respectively, for both analytical runs. Thus, a region with similar Fe and P CPS will contain approximately 200-fold more P atoms than Fe atoms.

Pearson product-moment correlation coefficients ($R_{Fe/P}$, $R_{Fe/S}$) were subsequently used quantify spatial correlations between Fe and P, and Fe and S. Temporal changes in spatial

correlations between Fe and P or S were analyzed by linear regression. All statistical analyses were carried out by the software package JMP (SAS, Cary, NC, USA).

Results

The spatial distributions of Fe in 38 trichome sections from Exp. I and 26 trichomes sections from Exp. II (Table 1) were examined using two dimensional SXRF element distribution maps and compared to maps of S and P, and light micrographs (e.g. Fig. 2-5, S1). Trichomes showed significant heterogeneity in the distributions of Fe, S, and P (Fig. 2A-5A). Some trichome sections (21 and 4 % of sections analyzed from Exp. I and Exp. II, respectively; Fig. 2A-4A) were enriched in Fe and S but contained relatively little P in comparison to neighboring trichome regions. Based on light micrographs, trichome sections with increased Fe and S and decreased P in comparison to neighboring trichome regions contained approximately 15 to 25 contiguous cells. In other trichome sections, enrichment in P was observed in less than 10 contiguous cells (Fig. 5A). Other trichome sections were split into low-P and high-P subsections (Fig. S1A, C, D), or did not show any element heterogeneity (Fig. S1B). Since the samples were treated with an oxalate/EDTA solution prior to mounting, the elements measured with SXRF are assumed to be located within the cells and not extracellularly adsorbed. However, in a few sections Fe seems to be adsorbed extracellularly (Fig. S1D, E). Such extracellular Fe enrichment did not correspond to enrichment in S, and the increase in Fe did not follow the outline of the trichome (Fig. S1D, E).

Element distribution patterns were quantified along the long axis of trichomes (Fig. 2B-5B, S1). In most Fe- and S-enriched regions, concentrations of Fe and S increased approximately 2-fold relative to non-enriched regions in the same trichome (Exp. I, Fig. 3B -4B). The exception is one trichome collected from Exp. II in which Fe increased ca. 12-fold with only a minor increase in S (Fig 2B). Furthermore, the increases of S and Fe were slightly offset to each other in this particular trichome (Fig 2A, B). In comparison, trichome regions with higher P were typically

enriched 2- to 6-fold relative to surrounding cells (e.g. Fig 5). Increases in P concentration were usually observed to be independent of variations of either Fe or S.

Spatial relationships between Fe and P or S were assessed using scatterplots extracted from one dimensional cross sections (Fig 2C, D-5C, D, S1) with the strength of correlations between elements quantified using the Pearson product-moment correlation coefficient (hereafter correlation coefficient or R). Spatial correlations between Fe and S or P varied between trichome sections, including between different sections of the same trichome (Fig. S1). Correlation coefficients were positive in most of the sections collected from Exp. II (Fig. 6) Additionally, Fe was positively correlated with S in nearly all sections analyzed from Exp. I (Fig. 6). Iron was more closely correlated with S than with P in 84% of sections in Exp. I (Table 1). In contrast, Fe was more correlated with S in only half of the Exp. II sections (Table 1). The mode of the correlation coefficients between Fe and S ($R_{Fe/S}$) in Exp I, and between Fe and S ($R_{Fe/S}$) and Fe and P ($R_{Fe/P}$) in Exp. II, was between 0.4 and 0.5 (Fig. 6). Mean (± stdev) correlation coefficients for these were 0.41 (± 0.33), 0.44 (± 0.27), and 0.44 (± 0.37), respectively. In contrast, the mode for $R_{Fe/P}$ from trichome sections collected during Exp. I was lower (mean 0.037 ± 0.33). A small percentage of sections from both experiments (5-8%) had a negative correlation between Fe and S. Negative correlations between Fe and P were more common (8-38%). Correlations between Fe and S were not strongly negative ($R_{Fe/S}<0.35$) in either experiment, yet Fe and P were strongly negatively correlated in 21 and 4 % of sections from Exp. I and Exp. II, respectively (Table 1). A total number of 8 trichomes (21%) were found to have sections enriched in Fe in Exp. I, and 6 of these trichomes had a moderate to strong positive correlation between Fe and S ($R_{Fe/S} > 0.35$) and a moderate to strong negative correlation between Fe and P ($R_{Fe/P} > 0.35$). However, two of

these Fe-rich sections had a weaker positive correlation between Fe and S but still a strong negative correlation between Fe and P.

Comparing the strength of the correlations between Fe and S and Fe and P in the same trichome revealed some common features. Two-thirds of analyzed trichomes fall into one of the following four groups (Table 1):

I) Fe was moderate to strong positively correlated with both P and S ($R_{Fe/P}$, $R_{Fe/S}$ > 0.35). This was observed in 18 and 54 % of sections from Exp. I and Exp. II, respectively.

II) Fe was not strongly correlated with either P or S (-0.35< $R_{Fe/P}$, $R_{Fe/S}$<0.35). This was the case for 29 and 12 % of sections from Exp. I and Exp. II, respectively.

III) Fe was moderate to strong positively correlated with S and moderate to strong negatively correlated with P ($R_{Fe/P}$ < -0.35 & $R_{Fe/S}$ >0.35). This was observed for 16 and 4 % of sections from Exp. I and Exp. II, respectively.

IV) In none of the analyzed sections was Fe negatively correlated with both P and S.

Changes in element distributions during the diurnal cycle were assessed by comparing temporal changes in correlation coefficients. Linear regressions of the correlation coefficients against time were used to test for significance of the temporal changes. A wide distribution of correlation coefficients was observed for trichomes collected from both growth phases at most sampling points (Fig. 6). No significant temporal changes were observed in the mean correlation between Fe and S for either experiment (linear regression slope $p > 0.25$), nor for the correlation between Fe and P for trichomes collected during Exp. I ($p = 0.12$) (Fig. 7). However the correlation between Fe and P for trichome sections collected during Exp. II decreased

significantly during the light period ($R^2 = 0.443$, $p = 0.0014$) and increased again during the dark period (Fig. 7).

Discussion

The relationship between Fe availability and N fixation in the ocean has significant impact on the large-scale function of the oceans [23], and *Trichodesmium* has been identified as a major contributor to N fixation in the global ocean.[2a, 24] Thus, the cellular interactions of Fe and *Trichodesmium* are of keen interest.[11, 15, 25] Previous studies have mapped the spatial distributions of nitrogenase [3a], C and N[8] in cultured *Trichodesmium* and the distributions of Fe in field populations[14], and here we provide the first measurements of the spatial distribution of Fe in cultured *Trichodesmium*. Similar to field populations, Fe was not evenly distributed along trichomes. However, field populations of *Trichodesmium* showed an even distribution of P and S, while cultured *Trichodesmium* showed a high degree of variance between P and S concentrations along trichomes. These heterogeneous distributions suggest different physiological functions occur in the different cell regions. Increases in Fe are accompanied by increases in S, while P is often lower in trichome sections with elevated Fe. Although we did not find any evidence for temporal changes in the correlation between Fe and S, such changes were observed between Fe and P, with a decreasing correlation during the light period and an increasing correlation during the dark period. This suggests that *Trichodesmium* may spatially re-allocate elements over time to satisfy its biochemical demand.

Iron, S, and P are major element constituents of different cellular compounds.[26] Iron is the most abundant trace metal in *Trichodesmium* and is required for many processes including C- and N_2-fixation, chlorophyll synthesis, and electron transport during photosynthesis and respiration. Nitrogenase represents the largest Fe requirement in *Trichodesmium* [11, 15], and therefore Fe distribution is likely driven by the distribution of nitrogenase. Nitrogenase contains also at least similar number of S than Fe atoms. The Fe-protein of nitrogenase entails a Fe_4S_4

cluster, and the MoFe-protein consists of a P cluster with an Fe_8S_7 center and a M cluster with a $[MoFe_7S_9X]$ (X = C, N, O) stoichiometry.[27] Sulfur is also present in Fe-S clusters of many Fe proteins, in amino acids such as cysteine and methionine, in glutathione, and in cytochrome c.[26a] Fe-S clusters contribute to electron transfer, substrate binding, storage, regulation of gene expression and enzyme activity.[26a, 28] Additionally, S can also be present in sulfolipids in *Trichodesmium*[29], replacing phospholipids when *Trichodesmium* is P limited.[29] P is also a constituent of ATP[26a, 30] and can be allocated in polyphosphate (polyP) storage molecules in phytoplankton such as *Trichodesmium*.[31] However, most P is probably contained in nucleic acids.[30] In contrast to S, P-containing compounds do not typically contain Fe. In general, each element (Fe, S, and P) represents a different group of cellular compounds.

The observed distributions of Fe within trichomes likely indicate regions of elevated nitrogenase. Such regions were only observed in 21% of the sections analyzed, and the Fe content usually increased 2-fold in these elevated Fe regions, although 12-fold in one trichome region (Exp. II). Trichome regions elevated in Fe contained up to 25 contiguous cells. This Fe elevation in multiple contiguous cells is comparable to the makeup of diazocysts, which have increased nitrogenase in up to 30 contiguous cells in 1-4 trichome sections.[6, 9a, 13a] We did not observe multiple Fe-rich trichome sections in the same filament, but these may have been present in unanalyzed sections. Other studies have shown that only 5-35% of cells are diazocytes.[5-6, 32] Given our partial sampling of each trichome, the numbers reported here should be considered a conservative estimate of cell regions elevated in Fe (and presumably nitrogenase).

Contrasting distributions of P and S suggest proteomic adjustments in Fe-rich sections. Trichome sections elevated in Fe also contained more S but less P than non Fe-rich regions of the same trichome. Cells containing nitrogenase should have higher cellular concentrations of Fe

and S because nitrogenase contains at least similar numbers of Fe and S atoms.[27] Given the 90-fold sensitivity difference between Fe and S, one would expect a far greater increase in the fluorescence signal for Fe than for S for a given amount of nitrogenase. Therefore, our data indicate larger increases in S than Fe in the Fe-rich sections. Consequently, the increased Fe concentration might be explained by the presence of nitrogenase, but other cellular changes must drive changes in the overall S and P content of these Fe-rich sections. Proteomic analyses have shown a 50-fold higher expression of the Fe storage DPS protein (DNA binding protein from starved cells) in diazocyte-expressing *Trichodesmium* cultures. [33] It has been suggested that such proteins provide Fe for nitrogen fixation, [33] stress protection during stationary phase, [34] or other unknown functions in relation to diazocyte formation. [33] Other observed changes include increased levels of the respiratory enzyme cytochrome oxidase or glutamine synthetase.[35] However, the presence of either protein/enzyme would not result in a significant increase in S. Similarly, proteomic analysis revealed a higher expression of most components of the oxidative pentose phosphate pathway in diazocyte-containing trichomes, indicating an increase in P-containing proteins.[33] This would contradict our observation of reduced P in Fe-rich trichome sections. A potential mechanism that would increase S and concomitantly decrease P in cells is the replacement of phospholipids by sulfolipids. Such replacement has been observed for *Trichodesmium*, albeit under P limiting conditions.[29] Negative correlation of P and S was primarily observed in stationary phase cells (Exp. I), which could have been P limited. Furthermore, replacing phospholipids with sulfolipids may allow *Trichodesmium* to use the freed P for the generation of ATP and thereby supporting the energy expensive process of nitrogen fixation. Changes in the S:P ratio in Fe-rich sections might reflect a localized biochemical

adaptation to N fixation in these sections, rather than overall P limitation of the cultured trichomes.

Spatial P distributions are probably also related to changes in distribution of polyP storage bodies. PolyP phosphate storage in *Trichodesmium* has been reported to occur under P-replete as well as P-limiting conditions, and linked to luxury uptake or an overplus response, respectively.[31] The highest polyP concentration has been found in *Trichodesmium* grown under P-replete conditions and collected during stationary phase.[30] Although we do not have spectroscopic information[31], it is reasonable to link the sharp increases in P observed in some cells collected during stationary phase in Exp. I (e.g., Fig 4) to polyP storage granules. Such a sharp increase in P was not observed in contiguous cells with higher Fe and S. Previous ultrastructure analyses have shown that diazocytes may contain a reduced number of C- and N-storing cyanophycin granules.[5] However, other studies did not find decreases in cyanophycin granules in certain trichome sections, and also did not identify the presence of diazocytes.[8] The presence of P in polyP storage bodies in diazocytes has not been reported, and the dense appearance of diazocytes seems to indicate the absence of any larger structural compound, including polyP granules. This assumption is consistent with our observations of increased P levels only in cells outside of the trichome regions elevated in Fe.

Trichodesmium may have the ability to redistribute elements within trichomes[8]. Our results showed no significant change in correlation between Fe and S either during a diurnal cycle or between different stages of growth (Fig. 7; Exp. I versus Exp. II). In contrast, the correlation between Fe and P did change on a diurnal basis and between different stages of growth (Fig. 7; Exp. I versus Exp. II). Since the concentrations of Fe and P did not change within each section over the diurnal cycle (data not shown), the change in the correlation suggests an active

redistribution of elements within each section based on their biochemical need. Whether the observed temporal changes in correlation are related to a protective mechanism for nitrogenase[10b, c] is unknown, but these changes do not coincide with a temporal separation of C- and N_2-fixation during midday.[2a]

Differences in element correlations might characterize different stages of growth. The major observed difference between *Trichodesmium* in stationary (Exp. I) and exponential growth (Exp. II) was the overall lower correlation between Fe and P. This resulted in fewer trichomes having moderate to strong positive correlations between Fe and P (group I, Table 1), and more trichomes having a negligible or moderate to strong negative correlation between Fe and P (groups II and III, Table 1) in Exp. I than Exp. II. Although few studies have compared different *Trichodesmium* growth stages, our results are consistent with increased polyP storage in *Trichodesmium* during stationary phase.[31] It has been well described that genetic adaptation is central to survival in stationary phase, [36] and it has been suggested that polyP development helps in this period of adjustment to stress and deprivation.[37] Just the presence of polyP will weaken the correlation between Fe and P, because Fe is not expected to be bound to polyP. Furthermore, our data seem to indicate that diazocyte formation is more common during stationary phase than during exponential growth. Whether growth stage differences can explain the differences between even[7b, c] and localized nitrogenase[3a, 9a] distribution observed in different studies is unknown. At least one study has found similar diazocyte numbers in *Trichodesmium* trichomes collected during exponential growth or stationary phase. [4c] Although trichomes were sampled here from only one population for each growth condition, the observed differences in correlation and numbers of Fe-rich sections are real and may be indicative of different stages of growth.

Conclusion

Previous studies have shown that *Trichodesmium* is able to develop special cells with a unique chemical composition. Our data show intra-trichome distributions of Fe consistent with the hypothesis of localized nitrogenase enrichment in diazocytes. Our data also reveal that Fe-rich sections undergo other cellular changes that result in higher S and lower P concentrations. Whether such cellular changes are the result of modifications in the lipid composition requires further diazocyte-specific proteomic and concurrent metallomic analyses. Changes in element correlations may indicate spatial element reallocation within trichomes, but further comparisons between different growth conditions are necessary to substantiate these observations. Overall, these spatial analyses of the *Trichodesmium* metallome provide supporting information allowing for a further unravelling of the unique *Trichodesmium* physiology.

Reference

1. (a) N. Gruber, J. N. Galloway, *Nature,* 2008, **451**, 293-296; (b) J. N. Galloway, F. J. Dentener, D. G. Capone, E. W. Boyer, R. W. Howarth, S. P. Seitzinger, G. P. Asner, C. Cleveland, P. Green, E. Holland, *Biogeochemistry,* 2004, **70**, 153-226.

2. (a) D. G. Capone, *Science,* 1997, **276**, 1221-1229; (b) R. Dugdale, D. W. Menzel, J. H. Ryther, *Deep Sea Research,*1961, **7**, 297-300; (c) T. Saino, A. Hattori, *Deep Sea Research,* 1978, **25**, 1259-1263.

3. (a) I. Berman-Frank, P. Lundgren, Y.-B. Chen, H. Küpper, Z. Kolber, B. Bergman, P. Falkowski, *Science,* 2001, **294**, 1534-1537 (b) A. W. Thompson, J. P. Zehr, *Journal of Phycology* 2013, **49**, 1024-1035.

4. (a) B. Bergman, E. J. Carpenter, *Journal of phycology,*1991, **27**,158-165; (b) B. Bergman, G. Sandh, S. Lin, J. Larsson, E. J. Carpenter, *FEMS microbiology reviews,* 2013, **37**, 286-302; (c) S. Lin, S. Henze, P. Lundgren, B. Bergman, E. J. Carpenter, *Applied and environmental microbiology,* 1998, **64**, 3052-3058.

6. G. Sandh, L. Xu, B. Bergman, *Microbiology,* 2012, **158**, 345-352.

5. C. Fredriksson, B. Bergman, *Protoplasma,*1997, **197**, 76-85.

7. (a) H. W. Paerl, J. C. Priscu, D. L. Brawner, *Applied and environmental microbiology,* 1989, **55**, 2965-2975; (b) K. Ohki, *Journal of oceanography,* 2008, **64**, 211-216; (c) K. Ohki, Y. Taniuchi, *Journal of oceanography,* 2009, **65**, 427-432.

8. J. A. Finzi-Hart, J. Pett-Ridge, P. K. Weber, R. Popa, S. J. Fallon, T. Gunderson, I. D. Hutcheon, K. H. Nealson, D. G. Capone, *Proceedings of the National Academy of Sciences,* 2009, **106**, 6345-6350.

9. (a) R. El-Shehawy, C. Lugomela, A. Ernst, B. Bergman, *Microbiology,* 2003, **149**, 1139-1146; (b) J. Larsson, J. A. Nylander, B. Bergman, *BMC evolutionary biology,* 2011, **11**, 187.

10. (a) E. Andresen, J. Lohscheider, E. Šetlikova, I. Adamska, M. Šimek, H. Küpper, *New Phytologist,* 2010, **185**, 173-188; (b) H. Küpper, E. Andresen, S. Wiegert, M. Šimek, B. Leitenmaier, I. Šetlík, *Biochimica et Biophysica Acta (BBA)-Bioenergetics,* 2009, **1787**, 155-167; (c) H. Küpper, N. Ferimazova, I. Šetlík, I. Berman-Frank, *Plant physiology,* 2004, **135**, 2120-2133.

11. S. Whittaker, K. D. Bidle, A. B. Kustka, P. G. Falkowski, *Environmental microbiology reports,* 2011, **3**, 54-58.

12. D. Shi, S. A. Kranz, J.-M. Kim, F. M. M. Morel, *Proceedings of the National Academy of Sciences,* 2012, **109**, E3094–E3100.

13. (a) I. Berman-Frank, J. T. Cullen, Y. Shaked, R. M. Sherrell, P. G. Falkowski, *Limnology and Oceanography,* 2001, **46**, 1249-1260; (b) I. Berman-Frank, A. Quigg, Z. V. Finkel, A. J. Irwin, L. Haramaty, *Limnology and Oceanography,* 2007, **52**, 2260-2269; (c) A. Tovar-Sanchez, S. A. Sañudo-Wilhelmy, A. B. Kustka, S. Agustí, J. Dachs, D. A. Hutchins, D. G. Capone, C. M. Duarte, *Limnology and Oceanography,* 2006, **51**, 1755-1761.

14. J. Nuester, S. Vogt, M. Newville, A. B. Kustka, B. S. Twining, *Frontiers in Microbiology,* 2012, **3**, DOI: 10.3389/fmicb.2012.00150.

15. A. B. Kustka, S. A. Sanudo-Wilhelmy, E. J. Carpenter, D. Capone, J. Burns, W. G. Sunda, *Limnology and Oceanography,* 2003, **48**, 1869-1884.

16. (a) A. Tovar-Sanchez, S. A. Sañudo-Wilhelmy, *Biogeosciences,* 2011, **8**, 217-225; (b) A. Tovar-Sanchez, S. A. Sañudo-Wilhelmy, M. Garcia-Vargas, R. S. Weaver, L. C. Popels, D. A. Hutchins, *Marine Chemistry,* 2003, **82**, 91-99.

17. (a) H. Bothe, O. Schmitz, M. G. Yates, W. E. Newton, *Microbiology and Molecular Biology Reviews,* 2010, **74**, 529-551; (b) T. Kentemich, G. Danneberg, B. Hundeshagen, H. Bothe, *FEMS Microbiology Letters,* 1988, **51**, 19-24.

18. Y. B. Chen, J. P. Zehr, M. Mellon, *Journal of Phycology,* 1996, **32**, 916-923.

19. G. Benoit, K. S. Hunter, T. F. Rozan, *Analytical Chemistry,* 1997, **69**, 1006-1011.

20. B. S. Twining, S. B. Baines, N. S. Fisher, J. Maser, S. Vogt, C. Jacobsen, A. Tovar-Sanchez, S. A. Sañudo-Wilhelmy, *Analytical Chemistry,* 2003, **75**, 3806-3816.

21. S. Vogt, *Journal De Physique IV,* 2003, **104**, 635-638.

22. D. R. Núñez-Milland, S. B. Baines, S. Vogt, B. S. Twining, *Journal of Synchrotron Radiation,* 2010, **17**, 560-566.

23. (a) P. G. Falkowski, *Nature,*1997, **387**, 272-275; (b) P. G. Falkowski, R. T. Barber, V. Smetacek, *Science,* 1998, **281**, 200-206; (c) S. Dutkiewicz, B. A. Ward, F. Monteiro, M. J. Follows, *Global Biogeochemical Cycles,* 2012, **26**, GB1012, DOI: 10.1029/2011GB004039.

24. D. G. Capone, J. A. Burns, J. P. Montoya, A. Subramaniam, C. Mahaffey, T. Gunderson, A. F. Michaels, E. J. Carpenter, *Global Biogeochemical Cycles,* 2005, **19**, GB2024, DOI: 10.1029/2004GB002331

25. P. D. Chappell, J. W. Moffett, A. M. Hynes, E. A. Webb, *The ISME Journal,* 2012, **6**, 1728-1739.

26. (a) J. J. R. Fraústo da Silva, R. J. P. Williams, *The Biological Chemistry of the Elements*. 2nd ed.; Oxford University Press: New York, 2001; p 600; (b) B. S. Twining, S. B. Baines, *Annual Review of Marine Science,* 2013, **5**, 191-215.

27. Y. Ohki, K. Tatsumi, *Zeitschrift für anorganische und allgemeine Chemie,* 2013, **639**, 1340-1349.

28. R. Lill, *Nature,* 2009, **460**, 831-838.

29. B. A. S. Van Mooy, H. F. Fredricks, B. E. Pedler, S. T. Dyhrman, D. M. Karl, M. Koblížek, M. W. Lomas, T. J. Mincer, L. R. Moore, T. Moutin, M. S. Rappé, E. A. Webb, *Nature,* 2009, **458**, 69-72.

30. R. Sterner, J. Elser, Ecological stoichiometry: the biology of elements from molecules to the biosphere Princeton University Press. *Princeton, New Jersey* 2002.

31. E. D. Orchard, C. R. Benitez-Nelson, P. J. Pellechia, M. W. Lomas, S. T. Dyhrman, *Limnology and Oceanography,* 2010, **55**, 2161-2169.

32. G. Sandh, R. El-Shehawy, B. Díez, B. Bergman, *FEMS microbiology letters* 2009, **295**, 281-288.

33. G. Sandh, L. Ran, L. Xu, G. Sundqvist, V. Bulone, B. Bergman, *Proteomics,* 2011, **11**, 406-419.

34. S. Nair, S. E. Finkel, *Journal of bacteriology,* 2004, **186**, 4192-4198.

35. (a) B. Bergman, P. Siddiqui, E. Carpenter, G. Peschek, *Applied and environmental microbiology,* 1993, **59**, 3239-3244; (b) E. Carpenter, B. Bergman, R. Dawson, P. Siddiqui, E. Söderbäck, D. Capone, *Applied and environmental microbiology,* 1992, **58**, 3122-3129.

36. (a) R. Kolter, D. A. Siegele, A. Tormo, *Annual Reviews in Microbiology,* 1993, **47**, 855-874; (b) T. H. Tani, A. Khodursky, R. M. Blumenthal, P. O. Brown, R. G. Matthews, *Proceedings of the National Academy of Sciences,* 2002, **99**, 13471-13476.

37. (a) A. Kornberg, *Journal of Bacteriology,* 1995, **177**, 491-496; (b) N. N. Rao, A. Kornberg, *Journal of bacteriology,* 1996, **178**, 1394-1400.

Tables

Table 1. . Occurrence of trichomes within ranges of Pearson correlation coefficients.

Pearson correlation coefficient range	Group	Exp. I[a]	Exp. II[b]
$R_{Fe/P} < R_{Fe/S}$		84	50
$R_{Fe/P} < -0.35$		21	4
$R_{Fe/S} < -0.35$		0	0
$R_{Fe/P}, R_{Fe/S} > 0.35$	I	18	54
$-0.35 < R_{Fe/P}$ & $R_{Fe/S} < 0.35$	II	29	12
$R_{Fe/P} < -0.35$ & $R_{Fe/S} > 0.35$	III	16	4
$R_{Fe/P} > 0.35$ & $R_{Fe/S} < -0.35$	IV	0	0

[a]total number of tricome sections: 38, all numbers are reported as %
[b]total number of tricome sections: 26, all numbers are reported as %

Figure captions

Figure 1. Growth of Trichodesmium at different Fe concentrations. Arrow indicates when trichomes were sampled from the 200 nmol Fe L^{-1} culture for SXRF analysis.

Figure 2. A) Light micrograph and false-color element (P, S, and Fe) maps of a *Trichodesmium* trichome collected during exponential growth (Exp. II). The color scale for element maps is shown, with warmer colors indicating higher element concentrations. The color scale corresponds to a different concentration range for each element. Size of trichome (μm) is indicated by a black bar. The whole trichome was analyzed. B) One dimensional line plot along the main axis of the trichome shown above. Data were extracted from the entire visible section of the trichome mapped here. C) Scatter plots of pixel-specific element concentrations [CPS] of Fe versus P extracted from the 1D line plots. Black line: linear regression. D) Scatter plots of pixel-specific element concentrations [CPS] of Fe versus S extracted from the 1D line plots shown in B. Black line: linear regression.

Figure 3. A) Light micrograph and false-color element (P, S, and Fe) maps of a *Trichodesmium* trichome collected during stationary phase (Exp. I). The color scale for element maps is shown, with warmer colors indicating higher element concentrations. The color scale corresponds to a different concentration range for each element. Size of trichome section (μm) is indicated by a black bar. Ca. 25% of the whole trichome was analyzed. B) One dimensional line plot along the main axis of the trichome shown above. Data were extracted from the entire visible section of the trichome mapped here. C) Scatter plots of pixel-specific element concentrations [CPS] of Fe versus P extracted from the 1D line plots. Black line: linear regression. D) Scatter plots of pixel-

specific element concentrations [CPS] of Fe versus S extracted from the 1D line plots shown in B. Black line: linear regression.

Figure 4. A) Light micrographs, and false-color element (P, S, and Fe) maps of a *Trichodesmium* trichome collected during stationary phase (Exp. I). The color scale for element maps is shown, with warmer colors indicating higher element concentrations. The color scale corresponds to a different concentration range for each element. Size of trichome section (μm) is indicated by a black bar. Ca. 20% of the whole trichome was analyzed. B) One dimensional line plot along the main axis of the trichome shown above. Data were extracted from the entire visible section of the trichome mapped here. C) Scatter plots of pixel-specific element concentrations [CPS] of Fe versus P extracted from the 1D line plots. Black line: linear regression. D) Scatter plots of pixel-specific element concentrations [CPS] of Fe versus S extracted from the 1D line plots shown in B. Black line: linear regression.

Figure 5. A) Light micrographs, and false-color element (P, S, and Fe) maps of a *Trichodesmium* trichome collected during stationary phase (Exp. I). The color scale for element maps is shown, with warmer colors indicating higher element concentrations. The color scale corresponds to a different concentration range for each element. Size of trichome section (μm) is indicated by a black bar. Ca. 33% of the whole trichome was analyzed. B) One dimensional line plot along the main axis of the trichome shown above. Data were extracted from the entire visible section of the trichome mapped here. C) Scatter plots of pixel-specific element concentrations [CPS] of Fe versus P extracted from the 1D line plots. Black line: linear regression. D) Scatter plots of pixel-specific element concentrations [CPS] of Fe versus S extracted from the 1D line plots shown in B. Black line: linear regression.

Figure 6. Distributions of Pearson coefficients for correlations between Fe and S or P, extracted from 1D line plots along the main axis of analyzed trichomes.

Figure 7. Temporal distributions of Pearson coefficients for correlations between Fe and S or P, extracted from 1D line plots along the main axis of analyzed trichomes.

524 Figure 1

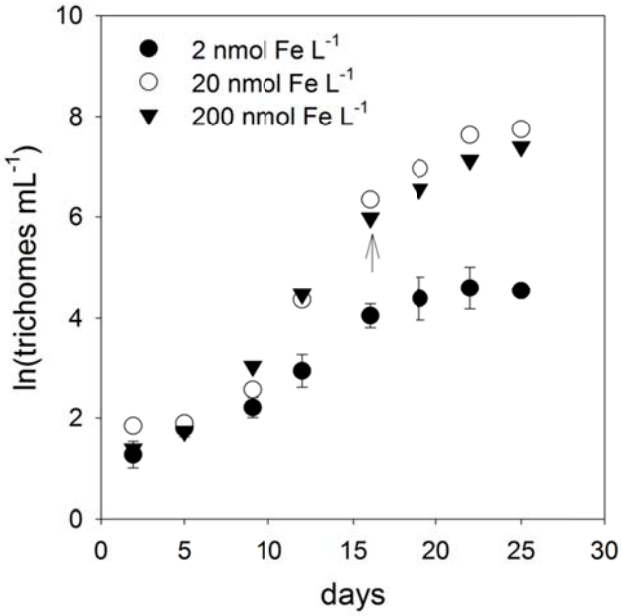

525

526

527

528 Figure 2.

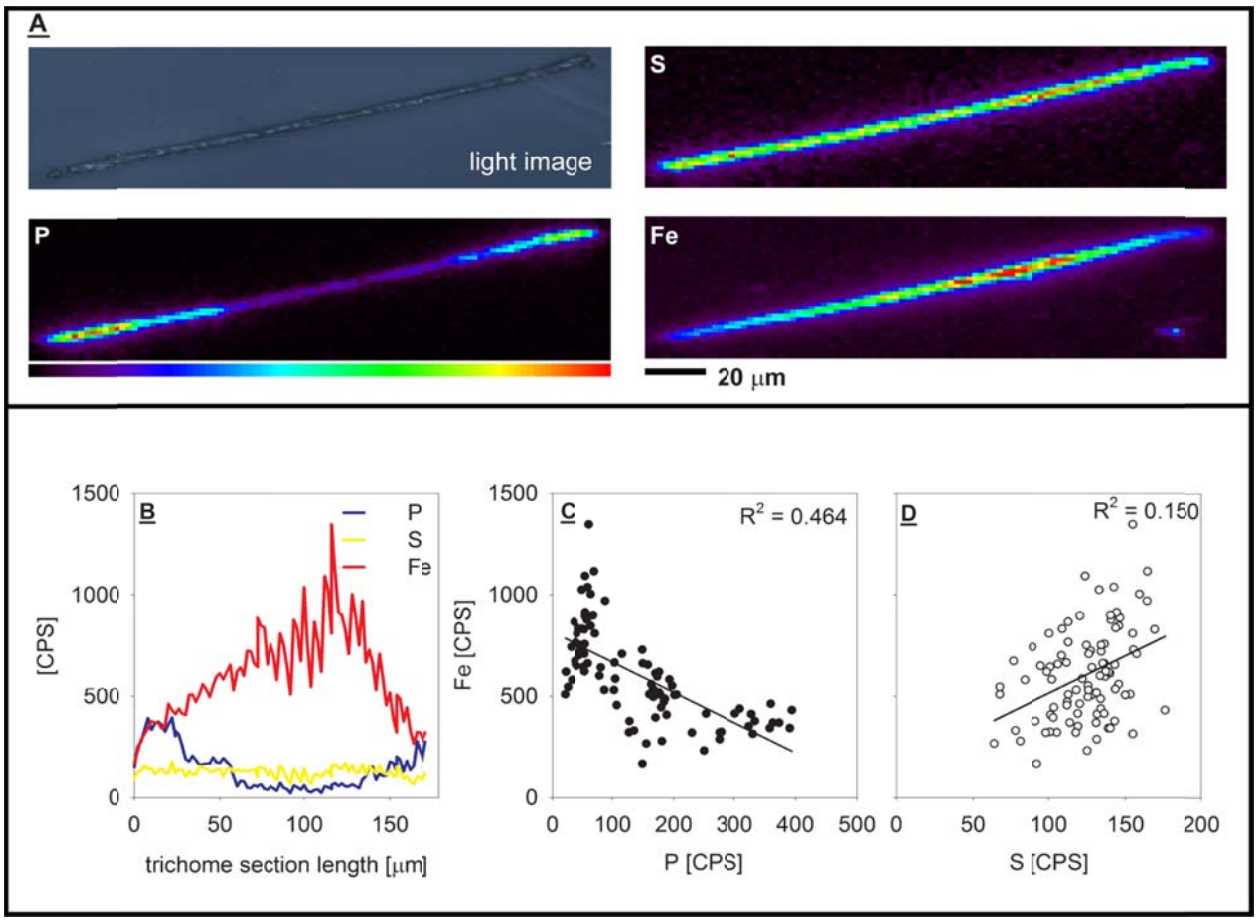

529

530

Figure 3.

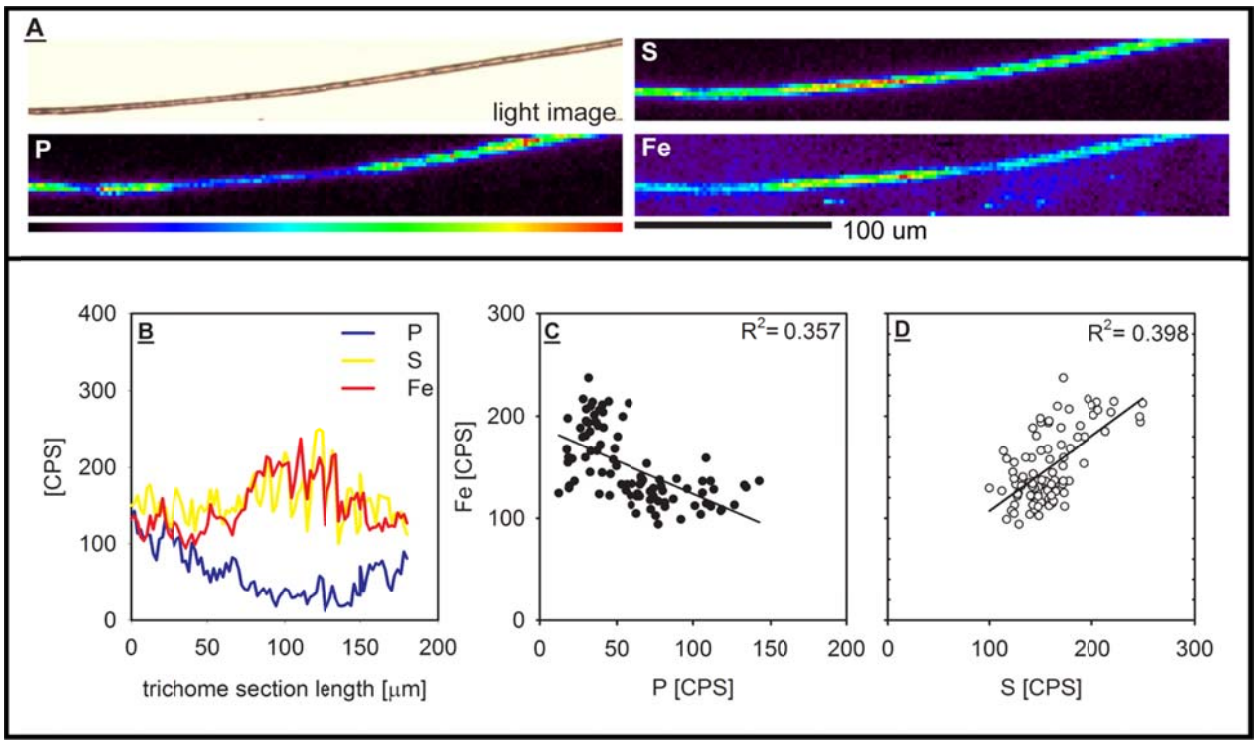

538 Figure 4.
539

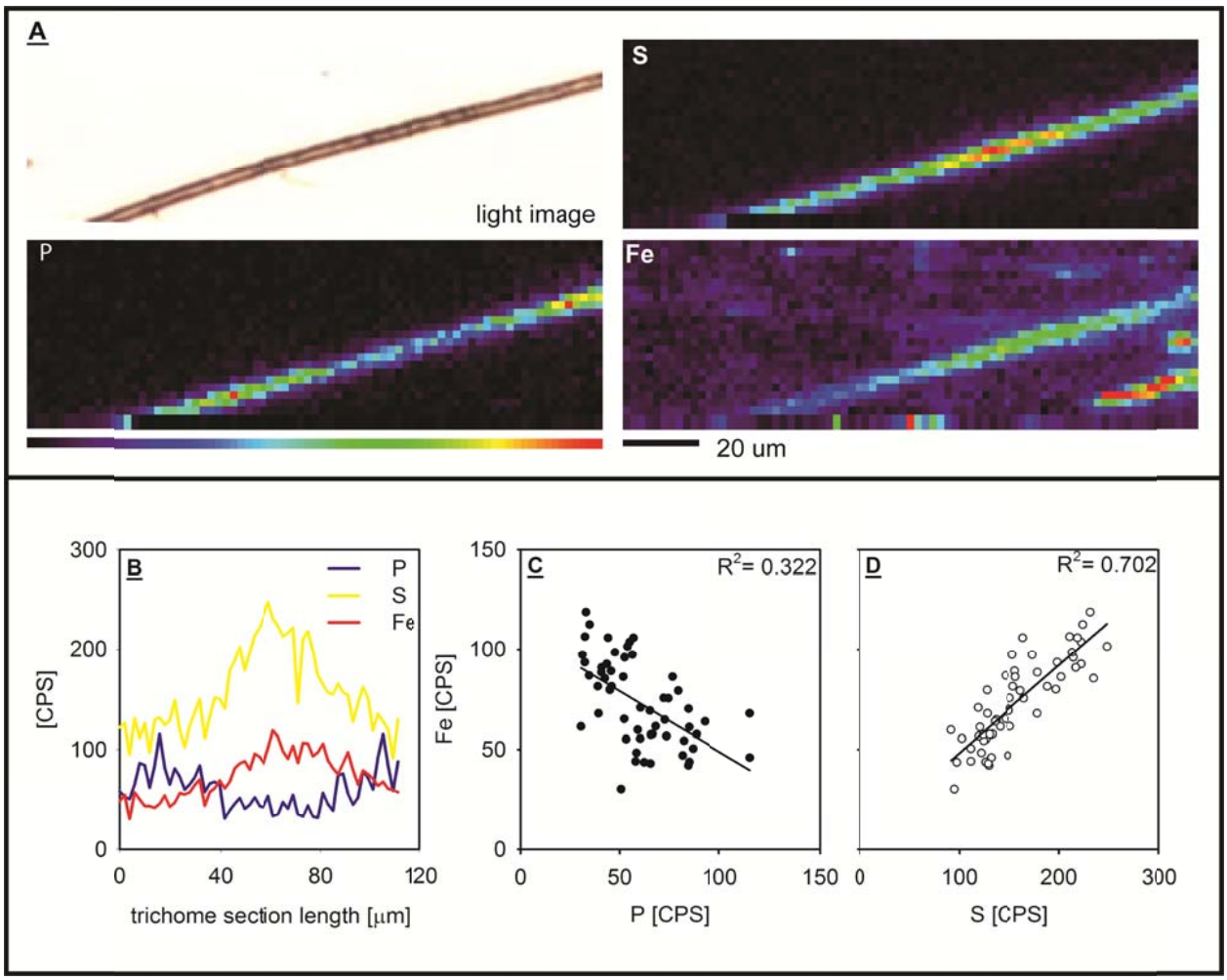

540
541
542

543 Figure 5.
544

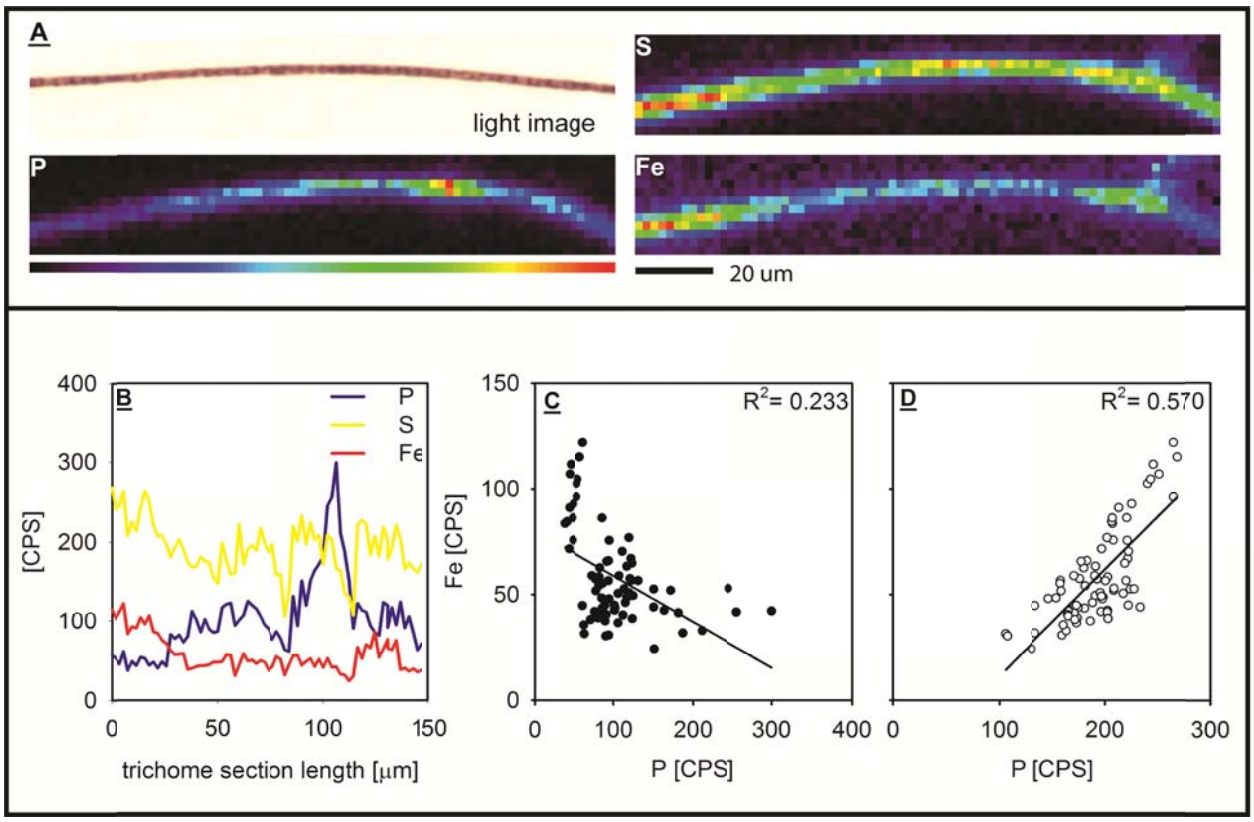

545
546
547

548 Figure 6.
549

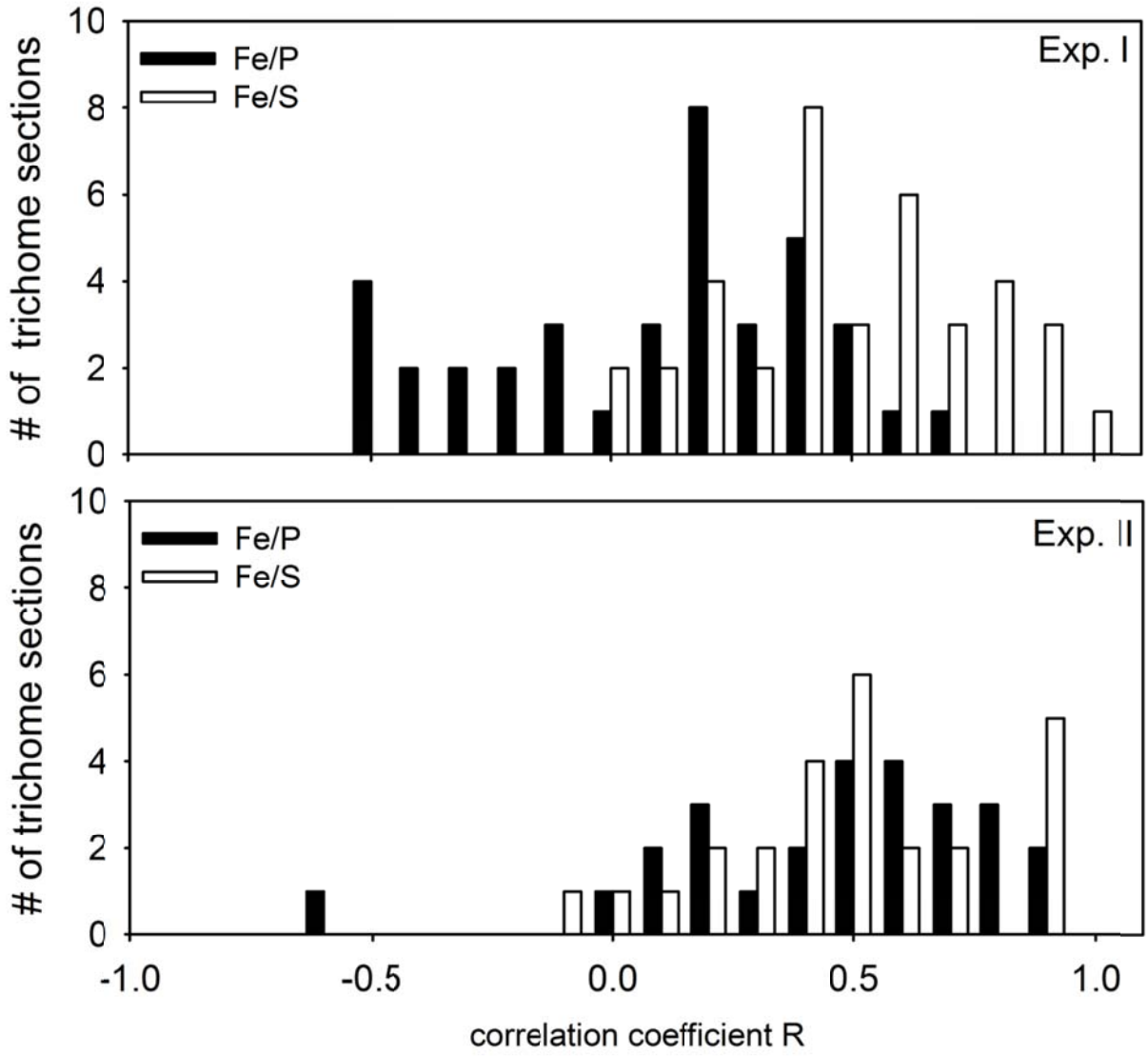

550
551
552

553 Figure 7.
554

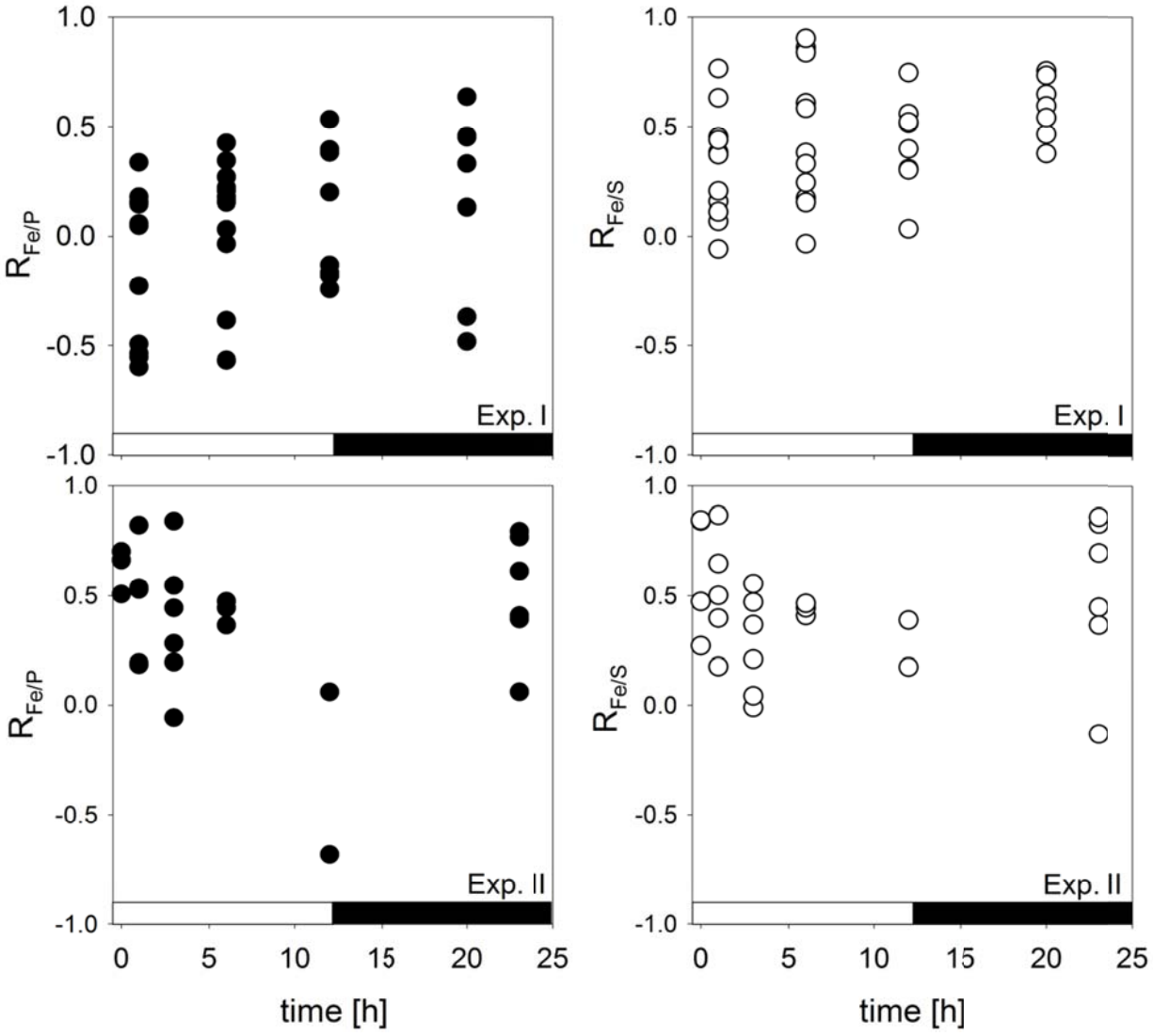

555
556